Original article
DOI: https://doi.org/10.18721/JPM.15312

EFFECTIVE DIFFUSION PROPERTIES OF A POLYCRYSTAL

D. M. Pashkovsky[1]✉, *K.P. Frolova*[2], *E. N. Vilchevskaya*[2]

[1] Peter the Great St. Petersburg Polytechnic University, St. Petersburg, Russia;

[2] Institute for Problems in Mechanical Engineering RAS, St. Petersburg, Russia

✉ mr.vivivilka@icloud.com

Abstract. The paper deals with the calculation of polycrystalline material effective diffusion coefficients. The polycrystalline material has been simulated by two-phase composite consisting of matrix and spheroidal inhomogeneities. The Mori – Tanaka scheme was used to account interactions between inhomogeneities. The proposed simulation took into account the effect of segregation as well. The paper put forward two models to describe the polycrystalline material. The former considered grains to be inhomogeneities, and grain boundaries to be a material matrix. The latter, in contrast, did the grain boundaries to be inhomogeneities, and the grains to be a material matrix. The simulation results were compared with experimental data. The importance of taking into account the segregation parameter when calculating effective diffusion coefficients of polycrystalline material was shown.

Keywords: two-phase composite, polycrystalline material, Mori – Tanaka scheme, effective diffusion properties, segregation effect

Funding: The reported study was funded by Russian Science Foundation (Project No. 18–19–00160).

Citation: Pashkovsky D. M., Frolova K. P., Vilchevskaya E. N., Effective diffusion properties of a polycrystal, St. Petersburg Polytechnical State University Journal. Physics and Mathematics. 15 (3) (2022) 154–168. DOI: https://doi.org/10.18721/JPM.15312

Научная статья
УДК 536.2
DOI: https://doi.org/10.18721/JPM.15312

ЭФФЕКТИВНЫЕ ДИФФУЗИОННЫЕ СВОЙСТВА ПОЛИКРИСТАЛЛА

Д. М. Пашковский[1]✉, *К. П. Фролова*[2], *Е. Н. Вильчевская*[2]

[1] Санкт-Петербургский политехнический университет Петра Великого, Санкт-Петербург, Россия;

[2] Институт проблем машиноведения РАН, Санкт-Петербург, Россия

✉ mr.vivivilka@icloud.com

Аннотация. Работа посвящена определению эффективных коэффициентов диффузии поликристаллического материала, для описания которого используется модель двухфазного композита, состоящего из матрицы и сфероидальных неоднородностей. Для учета взаимодействия между неоднородностями используется схема Мори – Танаки. В модели также учтен эффект сегрегации. Предложены две модели описания поликристаллического материала. В первой зерна моделируются неоднородностями, а граница зерен матрицей; во второй модели, наоборот, граница зерен моделируется неоднородностями, а зерна – матрицей материала. Результаты моделирования сравниваются с экспериментальными данными. Показано, что важно учитывать параметр сегрегации при расчете эффективных коэффициентов диффузии поликристаллического материала.

Ключевые слова: двухфазный композит, поликристаллический материал, схема Мори – Танаки, эффективные диффузионные свойства, эффект сегрегации

Финансирование: работа выполнена при поддержке Российского научного фонда, проект № 00160–19–18.

Ссылка для цитирования: Пашковский Д. М., Фролова К. П., Вильчевская Е. Н. Эффективные диффузионные свойства поликристалла // Научно-технические ведомости СПбГПУ. Физико-математические науки. 2022. Т. 15. № 3. С. 154–168. DOI: https://doi.org/10.18721/JPM.15312

Introduction

Finding the effective diffusion coefficients of solids is a crucial problem in many areas of industry and construction. Gas diffusion in a solid may produce pores, cracks, or other micro-defects that may grow over time and lead to fracture of structural elements. For this reason, the concentrations of the diffusing substance should be taken into account in evaluations of strength properties of the material.

The main practical applications include measures for preventing hydrogen embrittlement in metals and alloys or fracture in thin films. Hydrogen embrittlement produces a decrease in the strength properties of the metal alloy due to hydrogen diffusion, subsequently leading to fracture of the material [1]. It is essential to account for this effect in structures engineered for hydrogen energy storage or fuel cells in hydrogen-powered vehicles. Thin films are understood here as thin layers of another material applied to structural elements. One of the most typical examples are anti-corrosion coatings. The presence of defects in such coatings can produce increased concentrations of the diffusing substance, breaching the insulation of metals from the aggressive environment.

This paper considers the problem on quantifying the diffusion coefficients of polycrystalline material, which is inhomogeneous and contains a large number of randomly oriented single crystals, each of which can have different chemical and physical properties.

The single crystal is also called a grain in the literature, and the space between single crystals is known as the grain boundary [2].

There are many different mathematical models for quantifying the diffusion coefficients of polycrystalline materials. For example, Hart [3] obtained volumetric bulk coefficients for the case when the material contains dislocations; an equation similar to the rule of mixtures was used. Another study by Barrer [4] relied on the similarities between the processes of thermal conductivity and diffusion to find the tensor of effective diffusion coefficients similar to the tensor of conductivity in the thermal conductivity problem. Additionally, a ratio between the effective characteristics and properties of the material components was obtained. Barrer's approach is also used in other studies [5, 6].

Zhang and Liu [7] found that the concentration in the diffusion problem is not a continuous function at the interface, in contrast to the temperature in the thermal conductivity problem. The reason for this is that the diffusing substance accumulates at the boundary or inside the inhomogeneities, so the concentration makes a jump. This phenomenon is known as the segregation effect. Belova and March [8, 9] introduce the segregation parameter into the Hart and Maxwell–Garnett equations to calculate the effective properties of a material consisting of grain boundaries and spherical grains. Knyazeva et al. [2] represent the Mori–Tanaka method and the Maxwell homogenization scheme in terms of tensors of contribution to diffusion, serving for calculating the effective diffusion coefficients of isotropic material consisting of spheroidal grains, which are inhomogeneities, and grain boundaries, which are a matrix. On the other hand, the effect of segregation was not taken into account in [2] at the stage when the fields were averaged. The effect of segregation was taken into account in [10] at all stages of solving the homogenization problem for a transversely isotropic material with pores, whose anisotropy is due to the geometry of the microstructure.

The goal of our paper is to compare two approaches to simulation of polycrystalline materials.

Within the first approach, the grains are simulated by inhomogeneities and the grain boundary by the matrix, and, vice versa, the grain boundary is simulated by inhomogeneities, and the grains by the material matrix within the second approach. The models are compared by constructing a tensor of effective diffusion coefficients $\mathbf{D}_{eff}$ using the results obtained in [10]. In this case, the tensor $\mathbf{D}_{eff}$ takes the same form for both models of material. The difference in the models is reflected in the quantitative values of the microstructural parameters used.

Problem statement

The goal we set is achieved in two stages. First, we select a model for describing the polycrystalline material (Fig. 1, I) that can best approximate the effective diffusion coefficients of the real material. Second, an expression should be constructed for the tensor $\mathbf{D}_{eff}$. The homogenization problem is solved for this purpose (Fig. 1, II). Let us now consider each of the stages in more detail.

Two models of a two-phase composite are considered to describe the polycrystalline material (Fig. 1):

matrix–grain boundary, inhomogeneities–grains (M1);

matrix–grains, inhomogeneities–grain boundary (M2).

The composite consists of a matrix of material and isolated inhomogeneities placed in it both models; however, the matrix of the material and the inhomogeneities have different physical properties.

Models M1 and M2 differ only in the values of microstructural parameters: the segregation parameter s and the ratio of semi-major axis of the spheroid γ (see Table). The distribution of heterogeneities is assumed to be isotropic.

The following boundary conditions are imposed at the interface between the matrix (+)/inhomogeneity (–) phases [8, 9]:

$$D_0 \left.\frac{\partial c(x)}{\partial n}\right|_{x\to\partial V_1+} = D_1 \left.\frac{\partial c(x)}{\partial n}\right|_{x\to\partial V_1-}, \qquad (1)$$

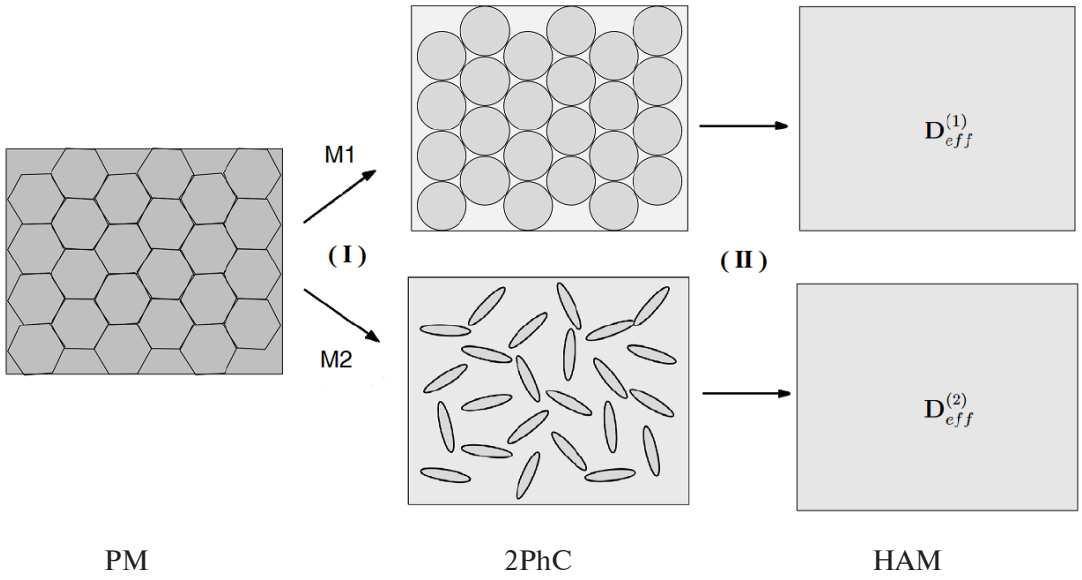

Fig. 1. Approximation scheme for polycrystalline material (PM) using Model 1 (M1) and Model 2 (M2) in two stages: modelling (I), homogenization (II); 2-phase composite (2PhC) and homogeneous anisotropic material (HAM) are shown; the corresponding tensors are given on the right

$$c(x)\big|_{x\to\partial V_1+} = sc(x)\big|_{x\to\partial V_1-}, \tag{2}$$

where D_0, D_1 are the diffusion coefficients of the material matrix and inhomogeneity, respectively; $c(x)$ is the concentration function with respect to the coordinate; ∂V_1 is the inhomogeneity boundary; **n** is the vector of the external normal to the inhomogeneity boundary, s is the segregation parameter.

Condition (1) stipulates that the fluxes at the interface be equal, while (2) describes the effect of segregation, i.e., the jump in concentration at the interface between the matrix and the inhomogeneity.

The segregation parameter s takes a value greater than unity in the model M1, and less than unity in the model M2. The reason for this is that the diffusing substance accumulates along the grain boundaries.

M1 considers spherical inhomogeneities, so $\gamma = 1$; the grain boundary in M2 is a highly oblate spheroid, so the parameter γ is taken in the range from 0.05 to 0.10.

The matrix and heterogeneities consist of an isotropic material with diffusion tensors taking the following form:

$$\mathbf{D}_0 = D_0\mathbf{E},\ \mathbf{D}_i = D_i\mathbf{E}, \tag{3}$$

where D_i is the diffusion coefficient of an ith heterogeneity, **E** is a single second-order tensor.

Table

Parameters of the models used and their values

Model	Segregation parameter s	Semi-major axes ratio γ for spheroid
1	$s > 1$	1.00
2	$s < 1$	0.05–0.10

$D_i < D_0$ for the model M1, since the diffusion coefficient of the grains is always less than that of the grain boundary. The opposite is true for the model M2: $D_i > D_0$.

After we select a model for describing the polycrystalline material, we construct an expression for the tensor of effective diffusion coefficients $\mathbf{D}_{eff}$. This requires a homogenization procedure, which consists in adopting a homogeneous continuous medium with anisotropic properties instead of an inhomogeneous medium [11].

The interaction between inhomogeneities is taken into account during homogenization. The Mori–Tanaka scheme is used for this purpose: its main principle is that each of the inhomogeneities is placed in a uniform field (either a concentration gradient or a diffusion flux acts as such a field in the context of the diffusion problem), equal to the average field with respect to the matrix of the material [12]. The Mori–Tanaka scheme is from the group of effective field methods, also including the widely used Maxwell and Kanaun–Levin schemes. However, unlike the latter two schemes, the Mori–Tanaka scheme does not have a singularity at a volume fraction of inhomogeneities equal to unity, so the model M1 can be used correctly, since the concentration of inhomogeneities in it is about 95–99%.

Contribution of isolated inhomogeneity

The contribution of isolated inhomogeneity to the effective properties of the material is determined following the steps similar to those described in our earlier paper [10]. The homogenization problem is solved introducing the concentrations and fluxes averaged over the volume. The averaging operation is denoted by the angle brackets and the subscript corresponding to the volume to be averaged.

It is assumed that the concentration $c(\mathbf{x})|_{\partial V} = \mathbf{G^0} \cdot \mathbf{x}$ is given at the boundary of the representative volume V considered. The concentration gradients $\langle \nabla c \rangle_V$ averaged over the representative volume V then amount to $\mathbf{G}^0$. At the same time, the flux $\langle \mathbf{J} \rangle_V \langle \mathbf{J} \rangle_V$, also averaged over the representative volume V, depends on the microstructure of the material.

The concentration gradient $\langle \nabla c \rangle_V$ is composed of the mean concentration gradient $\langle \nabla c \rangle_m$ of the substance, distributed in the matrix, the mean concentration gradient $\langle \nabla c \rangle_{in}$ of the substance, distributed within the inhomogeneity with a volume V_1, and the substance accumulated at the interface between the matrix and the inhomogeneity as a result of the segregation effect evolving:

$$\mathbf{G}^0 = \left\langle \nabla c \right\rangle_V = (1 - \frac{V_1}{V}) \left\langle \nabla c \right\rangle_m + \frac{V_1}{V} \left\langle \nabla c \right\rangle_{in} + \frac{1}{V} \int_{\partial V_1} \mathbf{n}(c_0 - c_1) d(\partial V_1). \tag{4}$$

In view of condition (2), expression (4) is converted to the following form:

$$\mathbf{G}^0 = \left\langle \nabla c \right\rangle_V = (1 - \frac{V_1}{V}) \left\langle \nabla c \right\rangle_m + s \frac{V_1}{V} \left\langle \nabla c \right\rangle_{in}. \tag{5}$$

The flux $\langle \mathbf{J} \rangle_V$ is continuous upon crossing the interface and consists of two components:

$$\left\langle \mathbf{J} \right\rangle_V = (1 - \frac{V_1}{V}) \left\langle \mathbf{J} \right\rangle_m + \frac{V_1}{V} \left\langle \mathbf{J} \right\rangle_{in}. \tag{6}$$

Taking into account Fick's first law, expression (6) takes the following form:

$$\left\langle \mathbf{J} \right\rangle_V = -(1 - \frac{V_1}{V}) \mathbf{D}_0 \cdot \left\langle \nabla c \right\rangle_m - \frac{V_1}{V} \mathbf{D}_1 \cdot \left\langle \nabla c \right\rangle_{in}. \tag{7}$$

In view of (5), expression (7) is converted to the form

$$\left\langle \mathbf{J} \right\rangle_V = -\mathbf{D}_0 \cdot \left\langle \nabla c \right\rangle_V - \frac{V_1}{V} (\mathbf{D}_1 - s\mathbf{D}_0) \cdot \left\langle \nabla c \right\rangle_{in}. \tag{8}$$

Next, $\langle \nabla c \rangle_{in}$ is expressed in terms of $\langle \nabla c \rangle_V$:

$$\langle \nabla c \rangle_{in} = \mathbf{\Lambda}_c \cdot \langle \nabla c \rangle_V = \mathbf{\Lambda}_c \cdot \mathbf{G}^0. \tag{9}$$

The tensor $\mathbf{\Lambda}_c$ is the solution of the Eshelby problem for diffusion. The expression for this tensor is obtained in [10] and has the form:

$$\mathbf{\Lambda}_c = [s\mathbf{E} + \mathbf{P} \cdot (\mathbf{D}_1 - s\mathbf{D}_0)]^{-1}, \tag{10}$$

where $\mathbf{P}$ is the Hill tensor.

In view of (9), Eq. (8) is converted to the following form:

$$\langle \mathbf{J} \rangle_V = -\left(\mathbf{D}_0 + \frac{V_1}{V} (\mathbf{D}_1 - s\mathbf{D}_0) \cdot \mathbf{\Lambda}_c \right) \cdot \mathbf{G}^0 = -\mathbf{D}_{eff} \cdot \mathbf{G}^0. \tag{11}$$

Thus, the inhomogeneous material consisting of the matrix and the inhomogeneity was replaced by a homogeneous anisotropic material with an effective diffusion tensor $\mathbf{D}_{eff}$.

Mori–Tanaka method

This section covers a generic material consisting of the matrix and n inhomogeneities. The interaction of inhomogeneities is described by the Mori–Tanaka scheme [12], outlined in Fig. 2. Each of the inhomogeneities is regarded as isolated and placed in an effective uniform field of the concentration gradient $\mathbf{G}^{eff}$, different from the one applied ($\mathbf{G}^0$) and equal to the average field over the material matrix $\langle \nabla c \rangle_m$.

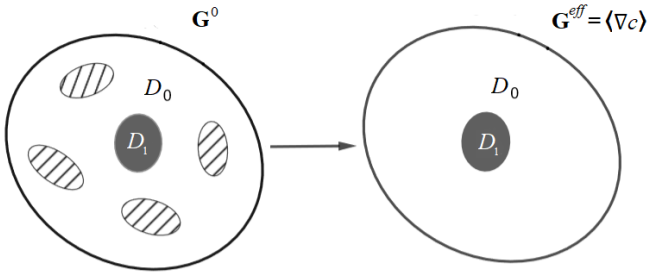

Fig. 2. Mori–Tanaka scheme:
interaction of isolated inhomogeneities (left) is taken into account by placing each of them in an effective field equal to the average over the material matrix (right)

The concentration gradient $\langle \nabla c \rangle_V$ is written as follows:

$$\mathbf{G}^0 = \langle \nabla c \rangle_V = \frac{1}{V} \sum_{i=1}^{n} V_i \langle \nabla c \rangle_{in}^i + (1-\varphi) \langle \nabla c \rangle_m + \frac{1}{V} \sum_{i=1}^{n} \int_{\partial V_i} \mathbf{N}_i (c_0 - c_i) d(\partial V_i), \tag{12}$$

where V_i, ∂V_i are the volume and boundary of an ith inhomogeneity; $\mathbf{N}_i$ is the normal to its boundary; φ is the volume fraction of inhomogeneities.

In view of boundary conditions (1) and (2), expression (12) is converted to the following form:

$$\mathbf{G}^0 = \langle \nabla c \rangle_V = s \frac{1}{V} \sum_{i=1}^{n} V_i \langle \nabla c \rangle_{in}^i + (1-\varphi) \langle \nabla c \rangle_m. \tag{13}$$

Expression (13) can be used to express $(1 - \varphi)\langle \nabla c \rangle_m$:

$$(1-\varphi) \langle \nabla c \rangle_m = \mathbf{G}^0 - s \frac{1}{V} \sum_{i=1}^{n} V_i \langle \nabla c \rangle_{in}^i. \tag{14}$$

Taking into account the Mori-Tanaka interaction, $\langle \nabla c \rangle^i_{in}$ is written as follows:

$$\left\langle \nabla c \right\rangle^i_{in} = \mathbf{\Lambda}^i_c \cdot \left\langle \nabla c \right\rangle_m, \tag{15}$$

where Λ^i_c is the concentration tensor for an ith heterogeneity.

The averaged flow is represented in the following form:

$$\left\langle \mathbf{J} \right\rangle_V = \frac{1}{V} \sum_{i=1}^{n} V_i \left\langle \mathbf{J} \right\rangle^i_{in} + (1-\varphi) \left\langle \mathbf{J} \right\rangle_m. \tag{16}$$

Next, expression (16) is transformed taking into account Fick's law:

$$\left\langle \mathbf{J} \right\rangle_V = -\frac{1}{V} \sum_{i=1}^{n} V_i \mathbf{D}_i \cdot \left\langle \nabla c \right\rangle^i_{in} - (1-\varphi) \mathbf{D}_0 \cdot \left\langle \nabla c \right\rangle_m. \tag{17}$$

In view of Eq. (14), expression (17) is converted to the following form:

$$\left\langle \mathbf{J} \right\rangle_V = -\mathbf{D}_0 \cdot \mathbf{G}^0 - \frac{1}{V} \sum_{i=1}^{n} V_i (\mathbf{D}_i - s\mathbf{D}_0) \cdot \left\langle \nabla c \right\rangle^i_{in}. \tag{18}$$

Relations (14) and (15) are used to obtain the expression for $\langle \nabla c \rangle^i_{in}$:

$$\left\langle \nabla c \right\rangle^i_{in} = \mathbf{\Lambda}^i_c \cdot [s \frac{1}{V} \sum_{i=1}^{n} V_i \mathbf{\Lambda}^i_c + (1-\varphi)\mathbf{E}]^{-1} \cdot \mathbf{G}^0. \tag{19}$$

Next, form (18) is converted to the following form taking into account expression (19):

$$\left\langle \mathbf{J} \right\rangle_V = -\mathbf{D}_0 \cdot \mathbf{G}^0 - \frac{1}{V} \sum_{i=1}^{n} V_i (\mathbf{D}_i - s\mathbf{D}_0) \cdot \mathbf{\Lambda}^i_c \cdot [s \frac{1}{V} \sum_{i=1}^{n} V_i \mathbf{\Lambda}^i_c + (1-\varphi)\mathbf{E}]^{-1} \cdot \mathbf{G}^0. \tag{20}$$

Taking into account Fick's law, we obtain the formula

$$\left\langle \mathbf{J} \right\rangle_V = -\mathbf{D}_{eff} \cdot \mathbf{G}^0. \tag{21}$$

Equalities (20) and (21) imply that the expression for $\mathbf{D}_{eff}$ takes the following form:

$$\mathbf{D}_{eff} = \mathbf{D}_0 + \frac{1}{V} \sum_{i=1}^{n} V_i (\mathbf{D}_i - s\mathbf{D}_0) \cdot \mathbf{\Lambda}^i_c \cdot [s \frac{1}{V} \sum_{i=1}^{n} V_i \mathbf{\Lambda}^i_c + (1-\varphi)\mathbf{E}]^{-1}. \tag{22}$$

Next, we convert expression (22) taking into account the averaging and equality $\mathbf{D}_i = \mathbf{D}_1$:

$$\mathbf{D}_{eff} = \mathbf{D}_0 + \varphi(\mathbf{D}_i - s\mathbf{D}_0) \cdot \left\langle \mathbf{\Lambda} \right\rangle_c \cdot [s\varphi \left\langle \mathbf{\Lambda} \right\rangle_c + (1-\varphi)\mathbf{E}]^{-1}. \tag{23}$$

Effective diffusion tensor

The Hill tensor for spheroidal heterogeneities takes the following form [11]:

$$\mathbf{P} = \frac{1}{D_0} (f_0(\gamma)(\mathbf{E} - \mathbf{nn}) + (1 - 2f_0(\gamma))\mathbf{nn}), \tag{24}$$

where the function $f_0(\gamma)$ is expressed as

$$f_0(\gamma) = \frac{(1-g(\gamma))\gamma^2}{2(\gamma^2-1)},\ g(\gamma) = \begin{cases} \dfrac{1}{\gamma\sqrt{1-\gamma^2}}\arctan\left(\dfrac{\sqrt{1-\gamma^2}}{\gamma}\right), & \gamma < 1 \\ 1/3, & \gamma = 1 \\ \dfrac{1}{2\gamma\sqrt{1-\gamma^2}}\log\left(\dfrac{\gamma+\sqrt{\gamma^2+1}}{\gamma-\sqrt{\gamma^2+1}}\right), & \gamma > 1. \end{cases} \quad (25)$$

The inverse second-order tensor is calculated by the Sherman–Morrison formula [14]. In general, it takes the following form:

$$\mathbf{B}^{-1} = (\mathbf{A} + \mathbf{n}_1\mathbf{n}_2)^{-1} = \mathbf{A}^{-1} - \frac{1}{1+\mathbf{n}_2\cdot\mathbf{A}^{-1}\cdot\mathbf{n}_1}(\mathbf{A}^{-1}\cdot\mathbf{n}_1\mathbf{n}_2\cdot\mathbf{A}^{-1}), \quad (26)$$

where $\mathbf{n}_1$, $\mathbf{n}_2$ are arbitrary vectors, **A**, **B** are second-order tensors.

In the case when **A** = **E**, Eq. (26) is converted to the form

$$\mathbf{B}^{-1} = (\mathbf{E} + \mathbf{n}_1\mathbf{n}_2)^{-1} = \mathbf{E} - \frac{1}{1+\mathbf{n}_2\cdot\mathbf{n}_1}\mathbf{n}_1\mathbf{n}_2. \quad (27)$$

We calculate the inverse tensor in expression (10) and obtain the following equation:

$$\left\langle [s\mathbf{E} + \mathbf{P}\cdot(\mathbf{D}_1 - s\mathbf{D}_0)]^{-1} \right\rangle = A_1\mathbf{E} + A_2\left\langle \mathbf{nn} \right\rangle, \quad (28)$$

where

$$A_1 = \frac{1}{s + \dfrac{f_0(D_1 - D_0 s)}{D_0}},$$

$$A_2 = \frac{D_0(3f_0 - 1)(D_1 - D_0 s)}{(D_1 - 2D_1 f_0 + 2D_0 f_0 s)(D_1 f_0 + D_0 s - D_0 f_0 s)}.$$

In the case when there is some predominant distribution of heterogeneities by orientation, it can be taken into account using the distribution function of the following form:

$$\psi_1(\upsilon,\xi) = \frac{1}{2\pi}((\xi^2+1)\exp(-\xi\upsilon) - \frac{1}{2}\exp(-\xi\pi)),\ \upsilon \in [0,\pi], \quad (29)$$

where ξ is the parameter for the spread in orientations, υ is the zenith angle in the spherical coordinate system.

Another distribution function is considered in [15], taking the following form:

$$\psi_2(\upsilon,\xi) = \frac{1}{2\pi}((\xi^2+1)\exp(-\xi\upsilon) + \xi\exp(-\xi\frac{\pi}{2})),\ \upsilon \in [0,\frac{\pi}{2}]. \quad (30)$$

Fig. 3 shows the influence of the parameter ξ on the spread in inhomogeneity orientations. If ξ = 0, all inhomogeneities are randomly oriented, so there is no preferential direction. As ξ increases, the orientations of the inhomogeneities tend to the given preferential direction.

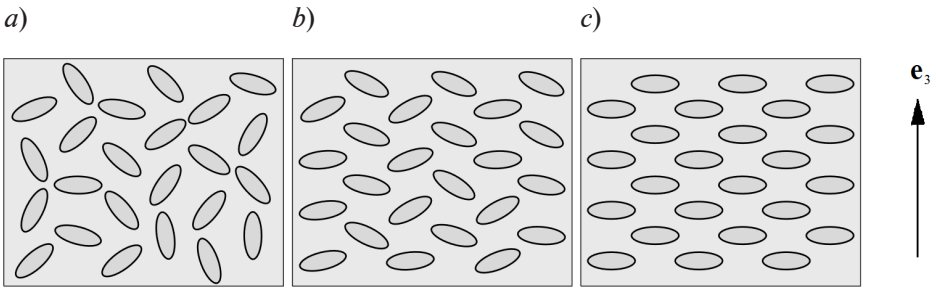

Fig. 3. Influence of parameter ξ on the spread in orientations of inhomogeneities relative to the predominant direction $\mathbf{e}_3$; **ξ = 0 (***a***)**, 7(*b*) 100 (*c*)

The orientation vector is given as follows in the spherical coordinate system:

$$\mathbf{n} = \cos(\theta)\sin(\upsilon)\mathbf{e}_1 + \sin(\theta)\sin(\upsilon)\mathbf{e}_2 + \cos(\upsilon)\mathbf{e}_3, \tag{31}$$

where $\mathbf{e}_1, \mathbf{e}_2, \mathbf{e}_3$ is the orthonormal basis; θ is the azimuthal angle in the spherical coordinate system.

The averaged tensor $\langle\mathbf{nn}\rangle$ accounting for the distribution function ψ_1 is calculated by the following formula:

$$\langle\mathbf{nn}\rangle = \int_0^{\pi}\int_0^{2\pi} \mathbf{nn}\psi_1(\upsilon,\xi)\sin(\varphi)d\theta d\upsilon. \tag{32}$$

As a result, we obtain the following expression for the dyad $\langle\mathbf{nn}\rangle$ (the preferred direction $\mathbf{e}_3$):

$$\langle\mathbf{nn}\rangle = \mathrm{N}_1\mathbf{e}_1\mathbf{e}_1 + \mathrm{N}_2\mathbf{e}_2\mathbf{e}_2 + \mathrm{N}_3\mathbf{e}_3\mathbf{e}_3. \tag{33}$$

The components of $\langle\mathbf{nn}\rangle$ take the following form:

$$\mathrm{N}_1 = \frac{1}{2\pi}\left(\frac{6\pi}{\xi^2+9} - \frac{2\pi}{3(\xi^2+9)}\xi^2\exp(-\pi\xi)\right), \tag{34}$$

$$\mathrm{N}_2 = \frac{1}{2\pi}\left(\frac{6\pi}{\xi^2+9} - \frac{2\pi}{3(\xi^2+9)}\xi^2\exp(-\pi\xi)\right), \tag{35}$$

$$\mathrm{N}_3 = \frac{1}{2\pi}\left(\frac{6\pi}{\xi^2+9} + \frac{2\pi\xi^2}{\xi^2+9} + \frac{4\pi}{3(\xi^2+9)}\xi^2\exp(-\pi\xi)\right). \tag{36}$$

In the case of the distribution function ψ_2, the tensor $\langle\mathbf{nn}\rangle$ is calculated from the formula

$$\langle\mathbf{nn}\rangle = \int_0^{\pi/2}\int_0^{2\pi} \mathbf{nn}\psi_2(\upsilon,\xi)\sin(\upsilon)d\theta d\upsilon. \tag{37}$$

The tensor $\langle\mathbf{nn}\rangle$ takes the form (33) but with different components:

$$\mathrm{N}_1 = \frac{1}{2\pi}\left(\frac{1}{\xi^2+9}\left(6\pi + 2\pi\xi\exp\left(-\frac{\pi}{2}\xi\right)\right) - \frac{\pi}{3}\xi\exp\left(-\frac{\pi}{2}\xi\right)\right), \tag{38}$$

$$\mathrm{N}_2 = \frac{1}{2\pi}\left(\frac{1}{\xi^2+9}\left(6\pi + 2\pi\xi\exp\left(-\frac{\pi}{2}\xi\right)\right) - \frac{\pi}{3}\xi\exp\left(-\frac{\pi}{2}\xi\right)\right), \tag{39}$$

$$\mathrm{N}_3 = \exp\left(-\frac{\pi}{2}\xi\right)\frac{\xi^2+3}{3(\xi^2+9)}\left(\xi + 3\exp\left(\frac{\pi}{2}\xi\right)\right). \tag{40}$$

The resulting expression for the tensor $\langle \mathbf{\Lambda} \rangle_c$ takes the following form:

$$\left\langle \mathbf{\Lambda} \right\rangle_c = \left\langle [s\mathbf{E} + \mathbf{P} \cdot (\mathbf{D}_1 - s\mathbf{D}_0)]^{-1} \right\rangle = A_1\mathbf{E} + A_2(\mathrm{N}_1\mathbf{e}_1\mathbf{e}_1 + \mathrm{N}_2\mathbf{e}_2\mathbf{e}_2 + \mathrm{N}_3\mathbf{e}_3\mathbf{e}_3). \quad (41)$$

The expression for $\mathbf{D}_{eff}$ (22) is converted to the following form taking into account Eq. (41):

$$\mathbf{D}_{eff} = D_0\mathbf{E} + (D_1 - sD_0)\varphi(B_1(\mathbf{e}_1\mathbf{e}_1 + \mathbf{e}_2\mathbf{e}_2) + B_2\mathbf{e}_3\mathbf{e}_3), \quad (42)$$

where the coefficients B_1 and B_2 follow the expressions:

$$B_1 = \frac{A_1 + A_2\mathrm{N}_1}{s\varphi(A_1 + A_2\mathrm{N}_1) + (1-\varphi)},$$

$$B_2 = \frac{A_1 + A_2\mathcal{N}_3}{s\varphi(A_1 + A_2\mathcal{N}_3) + (1-\varphi)}.$$

The constructed expression for the tensor of effective diffusion coefficients (42) is used for both models of polycrystalline material. The difference between the models is only in the numerical values of the microstructural parameters.

Results

Consider the components of the tensor $\mathbf{D}_{eff}$ as functions of various generalized microstructural parameters. The diffusion coefficient at the grain boundary is taken equal to $D_{gb} = 4 \cdot 10^{-2}$ m^2/s, and the diffusion coefficient of the grain is taken equal to $D_{gr} = 9 \cdot 10^{-5}$ m^2/s. The remaining microstructural parameters are given in the table above.

First, let us compare the influence of functions ψ_1 and ψ_2 (distributions of inhomogeneities by orientation) on the effective diffusion properties. The material is isotropic in the model M1, because the inhomogeneities are spherical, so the effective diffusion coefficients do not depend on the chosen distribution function. Fig. 4 shows the dependence for the components of the tensor $\mathbf{D}_{eff}$ on the scatter parameter ξ for model M2.

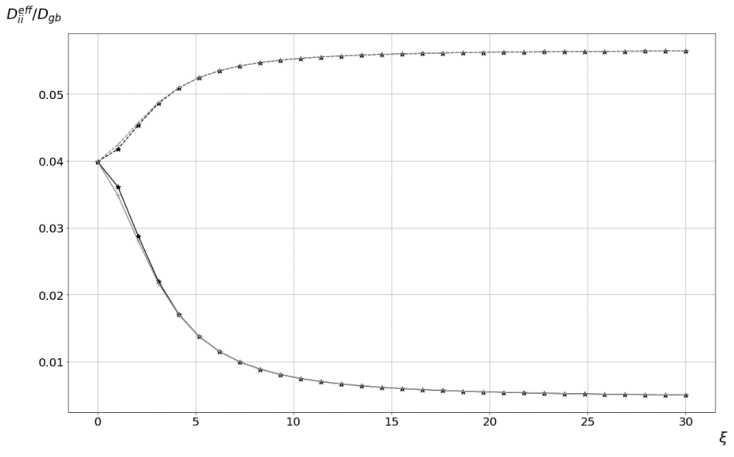

Fig. 4. Ratios D^{eff}_{11}/D_{gb} and D^{eff}_{33}/D_{gb} (components of the tensor $\mathbf{D}_{eff}$) as functions of the parameter ξ for the functions ψ_1 and ψ_2 (orientation distributions of inhomogeneities); model M2; $\gamma = 0.05$; $\varphi_{gr} = 0.5$; $s = 1$ (all 4 curves coincide)

The distribution functions ψ_1 and ψ_2 are found by Eqs. (29) and (30), respectively. Fig. 4 shows that the effective properties do not depend on the specific distribution function chosen to account for the spread in the orientation of the inhomogeneities. Next, we consider $\mathbf{D}_{eff}$ taking into account distribution function (29).

Notably, the chosen distribution function has no effect on the effective diffusion coefficients at $\xi = 0$, since this corresponds to the isotropic distribution of inhomogeneities. Suppose that the heterogeneities in the material are distributed isotropically ($\xi = 0$), so all components of the effective diffusion coefficient tensor $\mathbf{D}_{eff}$ are identical.

Fig. 5 shows the dependences of D^{eff}/D_{gb} on the grain volume fraction φ_{gr} for models M1 and M2. The dependences are plotted for volumes ranging from 0 to 1 to check whether the two models coincide in limiting cases at $s = 1$. The grain concentration φ_{gr} in real polycrystalline materials is close to unity.

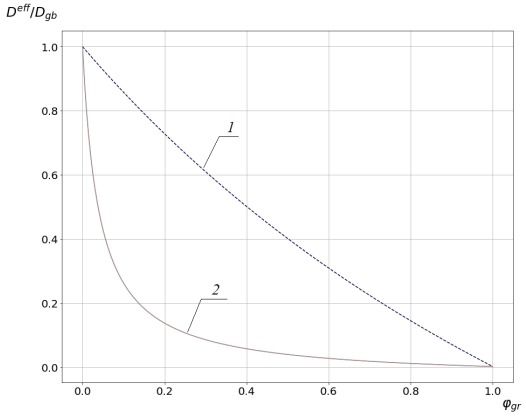

Fig. 5. Dependences of the ratio D^{eff}_{33}/D_{gb} (components of the tensor $\mathbf{D}_{eff}$) on the volume fraction of grains φ_{gr} for both models; $\gamma = 1.00$ for the model M1 (curve *1*) and $\gamma = 0.05$ for the model M2 (*2*); $s = 1.0$, $\xi = 0.0$

The two models coincide given the segregation parameter $s = 1$ at $\varphi_{gr} = 0$ and 1 (see Fig. 5). Furthermore, the behavior of the curves for models M1 and M2 is very different at any values of the volume fraction φ_{gr}, so the two models cannot be considered equivalent at the given values of parameters (see Table).

Fig. 6 shows the effect of the segregation parameter s on the effective diffusion coefficient at large volume fractions of the grains.

As evident from Fig. 6, variation in the segregation parameter has a more pronounced effect on the dependences for the model M2 than on those for the model M1. Both models show that the effective diffusion coefficient decreases with increasing segregation parameter. The segregation

a) *b*)

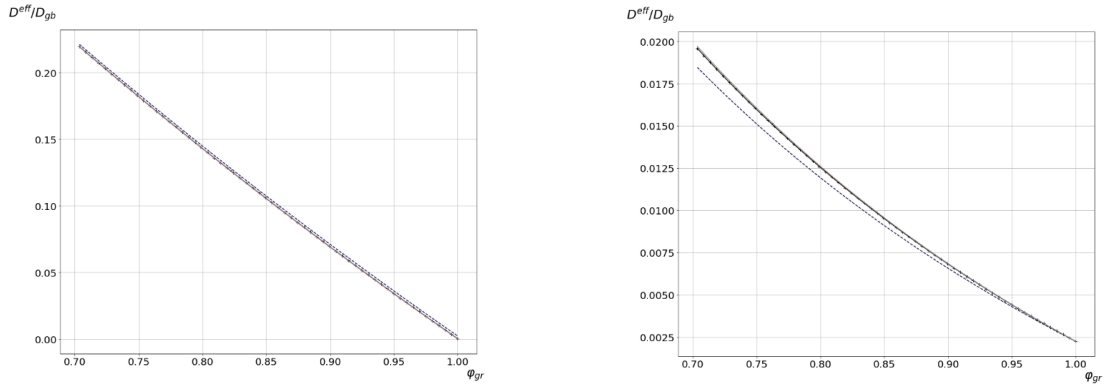

Fig. 6. Ratios D^{eff}_{33}/D_{gb} (components of the tensor $\mathbf{D}_{eff}$) as functions of the grain volume fraction φ_{gr} for models M1 (*a*) and M2 (*b*) at different values of the segregation parameter s: 1, 10, 100 (*a*) and 1, 0.1 and 0.01 (*b*);
curve $s = 1$ for M2 separated from the curves, which coincided; all curves coincided for M1

parameter has little influence on the effective diffusion coefficient in the model M1 at high concentrations of inhomogeneities.

Fig. 7 shows the dependence of D^{eff}_{33}/D_{gb} on the segregation parameter s with large volume fractions of grains (in the range from 95 to 99%). Evidently, the segregation parameter has little influence on the variation in the effective diffusion coefficient for both models, but a slight decrease in the diffusion coefficient is observed with increasing s.

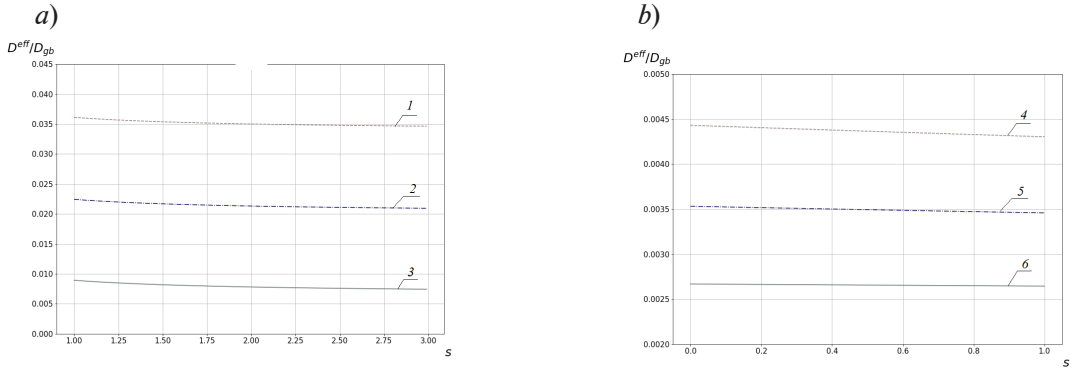

Fig. 7. Ratios D^{eff}_{33}/D_{gb} as functions of the segregation parameter s for models M1 (*a*) and M2 (*b*) at different values of the parameters γ and φ_{gr}; ξ = 0,0; γ = 1.00, φ = 0.95 (*1*), 0.97 (*2*), 0.99 (*3*) (*a*); γ = 0.05, φ = 0.05 (*4*), 0.03 (*5*), 0.01 (*6*) (*b*)

Verification of both models

This section compares the constructed mathematical models with the experimental data. Experimental data for the dependence of effective hydrogen diffusion coefficient in nickel on grain size d are given in [16].

The model M1 assumes spherical inhomogeneities to be grains with a diffusion coefficient $D_1 = 9 \cdot 10^{-14}$ m^2/s, and the grain boundary with $D_0 = 4 \cdot 10^{-10}$ m^2/s is taken as the matrix. The situation is reversed in the model M2: $D_0 = 9 \cdot 10^{-14}$ m^2/s, while $D_1 = 4 \cdot 10^{-10}$ m^2/s. The remaining microstructural parameters are given in the table.

The volume fraction of grain boundaries is calculated by the formula from [16]:

$$\varphi_{GB} = Ad^p,\ A = 8.138 \cdot 10^{-3},\ p = -0.636. \tag{43}$$

The volume fraction of grains is calculated by the following formula:

$$\varphi = 1 - \varphi_{GB} = 1 - Ad^p. \tag{44}$$

First we construct the dependence of D^{eff} on the grain size d for both models at $s = 1$.

It can be seen from Fig. 8 that the model M1 describes the experimental data fairly well. The approximation error of the experimental data is very large for the model M2, so only the model M1 is considered below.

Fig. 9 illustrates the influence of the segregation parameter s. Evidently, it is important that the segregation parameter is taken into account in the approximation of the effective diffusion coefficients. The best approximation of the experimental data is achieved at s values in the range from 1 to 2.

Thus, in practice, it is recommended to use the model M1 (matrix–grain boundaries, inhomogeneities–grains) rather than the model M2 (matrix–grains, inhomogeneities–grain boundaries) to approximate the diffusion coefficients of the polycrystalline material. We should note that a decrease in the values of effective diffusion coefficients is observed in the experimental data for grain sizes less than 0.1 μm, which can be associated with additional internal effects. It is established in [8] that the decrease in the value of the diffusion coefficient is due to an increase in the amount of solutes with a decrease in the grain size. Since this effect is not taken into account in the mathematical model of the material, both models also do not describe the effective diffusion properties for grain sizes less than 0.1 μm. Moreover, the segregation parameter does not significantly influence the effective diffusion coefficient in the case of spherical grains. The influence of the segregation parameter for spherical grains has not been investigated in this study; we plan to concentrate on this problem in our future research.

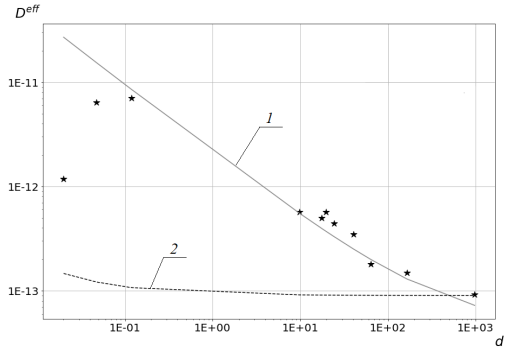

Fig. 8. Calculated (lines) and experimental (symbols) dependences of D^{eff} tensor components on d for models M1 (*1*) and M2 (*2*) at $s = 1$

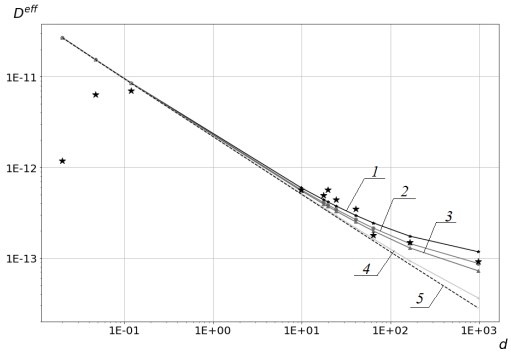

Fig. 9. Computational (lines) and experimental (symbols) dependences of the tensor component D^{eff} versus d for the model M1 at different s: 1.0 (*1*); 1.5 (*2*); 2.0 (*3*); 10 (*4*) and 100 (*5*)

Conclusion

The paper considers two approaches to describing polycrystalline material. The grains are simulated by inhomogeneities and the grain boundary by the matrix in the first case, and vice versa in the second case: the grain boundary is simulated by inhomogeneities, and the grains by the material matrix. The models used to approximate the effective diffusion coefficients of the polycrystalline material take into account the effect of segregation as well as the mutual effect of grains; the Mori–Tanaka scheme is applied. We have constructed an analytical approximation for the tensor of effective diffusion coefficients for the case of spheroidal inhomogeneities. We have verified the models using experimental data, establishing the importance of the segregation parameter for calculations of the effective diffusion coefficients.

REFERENCES

1. **Yakovlev Yu. A., Polyanskiy V. A., Sedova Yu. S., Belyaev A. K.,** Models of hydrogen influence on the mechanical properties of metals and alloys, PNRPU Mechanics Bulletin. (3) (2020) 136–160 (in Russian).

2. **Knyazeva A. G., Grabovetskaya G. P., Mishin I. P., Sevostianov I.** On the micromechanical modelling of the effective diffusion coefficient of a polycrystalline material, Phil. Mag. 95 (19) (2015) 2046–2066.

3. **Hart E. W.** Thermal conductivity, Acta Metallurgica. 5 (9) (1957) 597–605.

4. **Barrer R. M.,** Diffusion and permeation in heterogeneous media, In book: "Diffusion in polymers", Ed. by J. Crank and G. S. Park, Academic Press, London, 1968.

5. **Bell G. E., Crank J.** Influence of imbedded particles on steady-state diffusion, J. Chem. Soc. Farad. Trans. 70 (2) (1974) 1259–2732.

6. **Cussler E. L.,** Diffusion: mass transfer in fluid systems, Cambridge University Press, Cambridge, 2009.

7. **Zhang Y., Liu L.,** On diffusion in heterogeneous media, Am. J. Sci. 312 (9) (2012) 1028–1047.

8. **Belova I. V., Murch G. E.,** Diffusion in nanocrystalline materials, J. Phys. Chem. Solids. 64 (5) (2003) 873–878.

9. **Belova I. V., Murch G. E.,** The effective diffusivity in polycrystalline material in the presence of interphase boundaries, Phil. Mag. 84 (1) (2004) 17–28.

10. **Frolova K. P., Vilchevskaya E. N.,** Effective diffusivity of transversely isotropic material with embedded pores, Mater. Phys. & Mech. 47 (6) (2021) 937–950.

11. **Kachanov M., Sevostianov I.** Micromechanics of materials, with applications. Springer International Publishing AG (part of Springer Nature), Switzerland, 2018.

12. **Mori T., Tanaka K.** Average stress in matrix and average elastic energy of materials with misfitting inclusions, Acta Metallurgica. 21 (5) (1973) 571–574.

13. **Fricke H.,** A mathematical treatment of the electric conductivity and capacity of disperse systems. I. The electric conductivity of a suspension of homogeneous spheroids, Phys. Rev. 24 (5) (1924) 575–587.

14. **Sherman J., Morrison W. J.,** Adjustment of an inverse matrix corresponding to a change in one element of a given matrix, Ann. Math. Statistics. 21 (1) (1950) 124–127.

15. **Frolova K. P., Vilchevskaya E. N.,** Effective diffusion coefficient of a porous material applied to the problem of hydrogen damage, In book: “Advances in hydrogen embrittlement study”, Ed. by Polyanskiy V. A., Belyaev A. K., Book Ser. Advanced Structured Materials. Vol. 143, Springer International Publishing, Cham. (2021) 113–130.

16. **Oudris A., Creus J., Bouhattate J., et al.,** Grain size and grain-boundary effects on diffusion and trapping of hydrogen in pure nickel, Acta Materialia. 60 (19) (2012) 6814–6828.

СПИСОК ЛИТЕРАТУРЫ

1. **Яковлев Ю. А., Полянский В. А., Седова Ю. С., Беляев А. К.** Модели влияния водорода на механические свойства металлов и сплавов // Вестник Пермского национального исследовательского политехнического университета (ПНИПУ). Механика. 2020. № 3. С. 136–160.

2. **Knyazeva A. G., Grabovetskaya G. P., Mishin I. P., Sevostianov I.** On the micromechanical modelling of the effective diffusion coefficient of a polycrystalline material // Philosophical Magazine. 2015. Vol. 95. No. 19. Pp. 2046–2066.

3. **Hart E. W.** Thermal conductivity // Acta Metallurgica. 1957. Vol. 5. No. 9. Pp. 597–605.

4. **Barrer R. M.** Diffusion and permeation in heterogeneous media // Diffusion in polymers. Edited by J. Crank and G. S. Park. London: Academic Press, 1968. 259 p.

5. **Bell G. E., Crank J.** Influence of imbedded particles on steady-state diffusion // Journal of the Chemical Society, Faraday Transactions. 1974. Vol. 70. No. 2. Pp. 1259–2732.

6. **Cussler E. L.** Diffusion: mass transfer in fluid systems. Cambridge: Cambridge University Press, 2009. 631 p.

7. **Zhang Y., Liu L.** On diffusion in heterogeneous media // American Journal of Science. 2012. Vol. 312. No. 9. Pp. 1028–1047.

8. **Belova I. V., Murch G. E.** Diffusion in nanocrystalline materials // Journal of Physics and Chemistry of Solids. 2003. Vol. 64. No. 5. Pp. 873–878.

9. **Belova I. V., Murch G. E.** The effective diffusivity in polycrystalline material in the presence of interphase boundaries // Philosophical Magazine. 2004. Vol. 84. No. 1. Pp. 17–28.

10. **Frolova K. P., Vilchevskaya E. N.** Effective diffusivity of transversely isotropic material with embedded pores // Materials Physics and Mechanics. 2021. Vol. 47. No. 6. Pp. 937–950.

11. **Kachanov M., Sevostianov I.** Micromechanics of materials, with applications. Switzerland: Springer International Publishing AG (part of Springer Nature, 2018. 712 p.

12. **Mori T., Tanaka K.** Average stress in matrix and average elastic energy of materials with misfitting inclusions // Acta Metallurgica. 1973. Vol. 21. No. 5. Pp. 571–574.

13. **Fricke H.** A mathematical treatment of the electric conductivity and capacity of disperse systems. I. The electric conductivity of a suspension of homogeneous spheroids // Physical Review. 1924. Vol. 24. No. 5. Pp. 575–587.

14. **Sherman J., Morrison W. J.** Adjustment of an inverse matrix corresponding to a change in one element of a given matrix // The Annals of Mathematical Statistics. 1950. Vol. 21. No 1. Pp. 124–127.

15. **Frolova K. P., Vilchevskaya E. N.** Effective diffusion coefficient of a porous material applied to the problem of hydrogen damage // Advances in Hydrogen Embrittlement Study. Edited by Polyanskiy V. A., Belyaev A. K. Book Ser. Advanced Structured Materials. Vol. 143. Springer International Publishing, Cham., 2021. Pp. 113–130.

16. **Oudris A., Creus J., Bouhattate J., Conforto E., Berziou C., Savall C., Feaugas X.** Grain size and grain-boundary effects on diffusion and trapping of hydrogen in pure nickel // Acta Materialia. 2012. Vol. 60. No. 19. Pp. 6814–6828.

THE AUTHORS

PASHKOVSKY Dmitry M.
Peter the Great St. Petersburg Polytechnic University
29 Politechnicheskaya St., St. Petersburg, 195251, Russia
mr.vivivilka@icloud.com
ORCID: 0000-0002-2218-6649

FROLOVA Ksenia P.
Institute for Problems in Mechanical Engineering, RAS
61 Bolshoi Ave., V. Isl., St. Petersburg, 199178, Russia
kspfrolova@gmail.com
ORCID: 0000-0003-0376-4463

VILCHEVSKAYA Elena N.
Institute for Problems in Mechanical Engineering RAS
61 Bolshoi Ave., V. Isl., St. Petersburg, 199178, Russia
vilchevskaya_en@spbstu.ru
ORCID: 0000-0002-5173-3218

СВЕДЕНИЯ ОБ АВТОРАХ

ПАШКОВСКИЙ Дмитрий Максимович – *студент Физико-механического института Санкт-Петербургского политехнического университета Петра Великого.*
195251, Россия, г. Санкт-Петербург, Политехническая ул., 29
mr.vivivilka@icloud.com
ORCID: 0000-0002-2218-6649

ФРОЛОВА Ксения Петровна – м*ладший научный сотрудник Института проблем машиноведения РАН.*
199178, Россия, г. Санкт-Петербург, Большой проспект В. О., 61.
kspfrolova@gmail.com
ORCID: 0000-0003-0376-4463

ВИЛЬЧЕВСКАЯ Елена Никитична – *доктор физико-математических наук, ведущий научный сотрудник Института проблем машиноведения РАН.*
199178, Россия, г. Санкт-Петербург, Большой проспект В. О., 61.
vilchevskaya_en@spbstu.ru
ORCID: 0000-0002-5173-3218

Статья поступила в редакцию 08.04.2022. Одобрена после рецензирования 16.05.2022. Принята 16.05.2022.
Received 08.04.2022. Approved after reviewing 16.05.2022. Accepted 16.05.2022.